RESEARCH ARTICLE

Overlay Cognitive Radio Networks Enabled Energy Harvesting With Random AF Relays

DEEMAH H. TASHMAN[1], (Student Member, IEEE),
WALAA HAMOUDA[1], (Senior Member, IEEE),
AND JULES M. MOUALEU[2], (Senior Member, IEEE)

[1]Department of Electrical and Computer Engineering, Concordia University, Montreal, QC H3G 1M8, Canada
[2]School of Electrical and Information Engineering, University of the Witwatersrand Johannesburg, Johannesburg 2000, South Africa

Corresponding author: Walaa Hamouda (hamouda@ece.concordia.ca)

ABSTRACT In this paper, we investigate an overlay cognitive radio network (CRN) in which one user is selected among multiple secondary users (SUs) to harvest energy from primary transmissions using a time-switching protocol. Based on a power allocation scheme, the selected user utilizes a portion of the harvested energy to assist the primary user (PU) in forwarding its messages to a primary receiver, while the remaining portion is used to transmit its own information in exchange for this cooperation. Specifically, we evaluate the reliability of both the primary and secondary networks in terms of the outage probability. Moreover, both the time switching and power allocation factors that maximize the users' data rate are optimized.

INDEX TERMS Amplify-and-forward relaying, cognitive radio networks, energy harvesting, homogeneous Poisson point process (HPPP) distribution.

I. INTRODUCTION

The issue of spectrum under-utilization imposed by fixed spectrum allocation policies has been addressed through the development of cognitive radio (CR) technology [1]. With the explosive growth of wireless applications and services for the fifth generation (5G) and beyond networks, the demand for this technology has become crucial more than ever. There are two types of users in the context of cognitive radio networks (CRNs) viz. primary users (PUs) and second users (SUs) [2]. PUs are users that have been granted a license to operate in specified bands of the spectrum, whereas SUs are unlicensed users seeking to access the licensed bands. Three access modes can be exploited by the SUs to access the licensed bands viz. interweave, underlay and overlay [3], [4]. In the interweave mode, the SUs are allowed to access the licensed band through spectrum sensing as long as the bands remain vacant [5]. In the underlay mode, concurrent transmissions of both the PUs and the SUs are allowed on the condition that the interference caused by the latter is not beyond a threshold [6]. In the overlay approach, the SUs can access the licensed band

The associate editor coordinating the review of this manuscript and approving it for publication was Adamu Murtala Zungeru.

and in return, act as a relay node for the PU [7]. Relaying the PUs messages concurrently with the SUs messages in the overlay access mode consumes additional energy. As a result, the energy consumption issue in this paradigm needs to be addressed, especially for energy-constrained applications.

Energy harvesting (EH) has recently emerged as a viable solution to prolong the lifetime of energy-constrained systems [8], [9], [10]. Among the various EH techniques, simultaneous wireless information and power transfer (SWIPT) is an effective approach that is based on the notion that both the energy and information can be carried simultaneously through radio frequency (RF) signals [11], [12]. The implementation of the SWIPT technique can be accomplished either through power splitting (PS), time switching (TS), or antenna selection (AS) protocols. The time frame of a communication process adopting the TS protocol is mainly partitioned into two-time slots. During the first time slot, the receiver harvests energy from the surrounding received signals, while in the second time slot, the device forwards the messages to the intended destination using the harvested energy [13]. Integrating EH with CRNs has the advantage of improving both spectral efficiency and energy efficiency [14].

Recent studies have focused on implementing EH with CRNs to fulfill some criteria of future wireless networks. For instance, several reported works have investigated the integration of EH techniques in underlay CRNs (see [15], [16], [17], [18], and [19] and the references therein). From a security point of view, certain papers have focused on improving the security of underlay CRNs through EH, such as in [12], [14], [20], and [21], due to the elevation in the security concerns in 5G and beyond networks [22], [23]. In contrast to the underlay mode, the interference from the secondary transmissions on the primary network can be counteracted in the overlay mode. Additionally, the PU's performance is greatly improved due to SU relaying. Owing to these benefits, the adoption of EH-based on overlay CRNs is of utmost importance for the development of next generation wireless networks. However, few studies in the literature have paid attention to the analysis of EH-based overlay CRNs. For instance, the work in [24] considered a system wherein cooperation between a pair of SUs and PUs exists with the former users scavenging energy from the latter users through the PS protocol. The performance analysis of the underlying system was further studied in terms of the outage probability and energy efficiency. In [25], the authors investigated the performance of a system where the SU harvests energy by adopting a TS protocol for the transmission of the PU's information through a decode-and-forward (DF) relaying strategy. In return for this favor, the SU is allowed to access the licensed band for its own information transfer. In [26], Zhou et al. studied the optimized PS factor to improve the reliability of an overlay CRN where the PU harvests energy from the SUs' transmissions. In [27], Solanki et al. investigated the performance of a multiuser overlay CRN with EH based on a piece-wise linear model. Moreover, in [28], cooperation between SUs and PUs is explored, assuming a wireless-powered cooperative CRN and two multiple access algorithms for the SUs: non-orthogonal multiple access (NOMA) and time-division multiple access (TDMA). In this work, SUs assist PUs by wirelessly charging them in return for access to the licensed band. The PUs harvest energy from the SUs' transmissions and utilize it to forward their own transmissions to the PU destination. Similarly, in [29], a collaboration between PUs and SUs is implemented, in which PUs harvest energy from the transmissions of SUs while considering two strategies to coordinate the information transmission of the PU and the SU, namely subcarrier sharing (SS) and subcarrier exclusivity (SE).

Different from the above works, we consider an EH-based overlay CRN with multiple randomly distributed SUs [30]. To the authors' best knowledge, no prior work in the literature has investigated the impact of randomly placed SUs in the development of an energy- and spectrum-efficient system design, particularly for overlay access modes. This is the gap the proposed work aims to fill. The significance of assuming random positions for the SU relays will be shown in this paper. For instance, we allow k (the selected SU) to be variable and analyze its effect on overall performance. In addi-

tion, we examine the impact of the SUs relay density (ϕ) on system performance and the outage probability when PUs and SUs exist in regions dense with relays, as will be shown in the numerical results section. Moreover, assuming multiple SUs has a significant impact on the network continuity for both SUs and PUs. In certain cases involving several SUs, for instance, the first, second, and third closest SUs may no longer be available for transmission owing to unstable connections. Therefore, the fourth-closest SU may be utilized to relay the PUs' messages, ensuring that the connection is maintained. This highlights the necessity of randomly assigning locations to multiple relays. Herein, we propose an overlay CRN in which two PUs exchange information via one SU which acts as a relay, and is selected based on the Euclidean distance from a set of multiple randomly distributed SUs assuming a homogeneous Poisson point process (HPPP) distribution [31]. The reliability of both the primary and secondary networks is analyzed in terms of the outage probability. In addition, two optimization problems are formulated to (1) maximize the SUs' rate while ensuring the PUs' rate is maintained above a threshold; (2) to maximize the sum rate of both networks.

The rest of the paper is organized as follows; the system and channel models are presented in Section II. The outage probability analysis is studied in Section III. In Section IV, the optimization problems are presented. Section V includes and discusses the numerical results. Finally, conclusions are given in Section VI.

II. SYSTEM MODEL

Assume we have a primary user (PU) transmitter (PU-Tx) communicating with a PU receiver (PU-Rx) as shown in Figure 1 [30]. Due to the unavailability of a reliable link between the PUs, secondary users (SUs) are assumed to assist the primary users (PUs) in forwarding their messages in exchange for the use of a licensed band. We assume that M SUs are distributed according to a homogeneous Poisson point process (HPPP) with a density ϕ. One of the SUs is selected based on the kth nearest to PU-Tx. Moreover, the selected SU is permitted to harvest energy from PUs transmissions using the TS protocol via the channel h_{SR}. In addition, the selected SU performs as an amplify-and-forward (AF) relay, in which it amplifies the PUs' messages and forwards them to the PU destination along with its own messages to its receiver (SU-Rx). We assume that the SUs are distributed in an unbounded Euclidean space of dimension U.

Figure 2 shows the time frame of the TS-EH process. During the first time slot (ρT), the selected SU (R_k) harvests energy from the PUs messages with the energy harvested (E_s) given by

$$E_s = \frac{\rho \eta P_s T \, |h_{SR}|^2}{d^{PL}}, \tag{1}$$

where P_s is the transmission power at PU-Tx, $0 < \rho < 1$ is the time switching factor, d is the distance of a randomly distributed SU from PU-Tx, PL is the path loss exponent, η
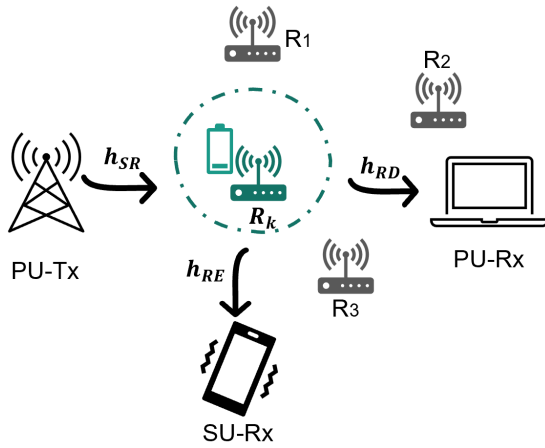
FIGURE 1. System model.

represents the energy conversion efficiency coefficient, and T is the transmission time slot. Using (1), the transmission power at R_k (P_R) is given by

$$P_R = \frac{E_s}{(1-\rho)T} = \frac{\rho\eta P_s |h_{SR}|^2}{(1-\rho)d^{PL}}. \tag{2}$$

The received message at the kth random SU is given by

$$y_{R,k} = \sqrt{\frac{P_s}{d^{PL}}}h_{SR}x_p + n_R, \tag{3}$$

where x_p is the PUs' transmitted message and n_R is the additive white Gaussian noise (AWGN) at the SU relay with a zero mean and a variance N_0. During the second time slot $((1-\rho)T)$, the selected SU (R_k) amplifies the PUs' messages and combines them with its own messages to be transmitted. These messages are received by both receivers, i.e., PU-Rx and SU-Rx. Given this, the received message at the PU-Rx is given by

$$y_D = \beta y_{R,k}h_{RD} + \sqrt{(1-\alpha)P_R}h_{RD}x_s + n_D, \tag{4}$$

where x_s is the transmitted SUs' messages and n_D is the AWGN at PU-Rx with a zero mean and a variance N_0. α represents a power allocation factor, in which αP_R is allocated to transmit the PUs messages, while the rest $((1-\alpha)P_R)$ is used to transfer the SUs' messages. Moreover, β is the amplification factor of R_k given by

$$\beta = \sqrt{\frac{\alpha P_R}{\frac{P_s g_{SR}}{d^{PL}} + N_0}}. \tag{5}$$

Without loss of generality, we assume that the noise variance (N_0) has a very low value compared to the fraction in the denominator of (5) at high signal-to-noise ratio (SNR), which is $\frac{P_s g_{SR}}{d^{PL}}$. That is, $\frac{P_s g_{SR}}{d^{PL}} \gg N_0$, and thus the term N_0 becomes negligible and can be ignored in the analyses [24], [32], [33], [34]. Hence, (5) can be approximated as

$$\beta \approx \sqrt{\frac{\alpha P_R}{\frac{P_s g_{SR}}{d^{PL}}}}. \tag{6}$$

Substituting (3) into (4), the received message at the PU-Rx is expressed as

$$y_D = \beta\sqrt{\frac{P_s}{d^{PL}}}h_{SR}x_p h_{RD} + \sqrt{(1-\alpha)P_R}h_{RD}x_s$$
$$+ \beta h_{RD}n_R + n_D. \tag{7}$$

Given (6) and (7), the instantaneous received signal-to-interference-plus-noise ratio (SINR) at PU-Rx is expressed as

$$\gamma_D = \frac{\beta^2 g_{RD}g_{SR}\frac{P_s}{d^{PL}}}{N_0 g_{RD}\beta^2 + g_{RD(1-\alpha)P_R+N_0}}. \tag{8}$$

It is worth mentioning that PU-Rx treats the SUs messages as interference. Hence, substituting (2) and (6) into (8) and performing mathematical manipulations yields

$$\gamma_D = \frac{a\frac{g_{RD}g_{SR}}{d^{PL}}}{bg_{RD} + c\frac{g_{RD}g_{SR}}{d^{PL}} + N_0}, \tag{9}$$

where $a = \frac{\alpha\rho\eta P_s}{1-\rho}$, $b = \frac{N_0\alpha\rho\eta}{1-\rho}$, and $c = \frac{(1-\alpha)\rho\eta P_s}{1-\rho}$. Moreover, the received message at SU-Rx is given by

$$y_S = \sqrt{(1-\alpha)P_R}h_{RE}x_s + n_s + \beta y_D h_{RE}, \tag{10}$$

where x_s is the SUs' transmitted messages and n_s is the AWGN at SU-Rx with a zero mean and a variance N_0. Using (10), the received SINR at SU-Rx is given as

$$\gamma_S = \frac{q\frac{g_{RE}g_{SR}}{d^{PL}}}{eg_{RE} + w\frac{g_{RE}g_{SR}}{d^{PL}} + N_0}, \tag{11}$$

where $q = \frac{(1-\alpha)\rho\eta P_s}{1-\rho}$, $e = \frac{N_0\alpha\rho\eta}{1-\rho}$, and $w = \frac{\alpha\rho\eta P_s}{1-\rho}$. Accordingly, the data rates achieved at PU-Rx and SU-Rx are given, respectively, as

$$R_P = (1-\rho)T \log_2(1+\gamma_D), \tag{12}$$
$$R_S = (1-\rho)T \log_2(1+\gamma_S). \tag{13}$$

We assume that all links follow the Rayleigh fading model. Hence, the channels power gain (g_m), for $m = SR, RD, RE$ follow the exponential distribution with λ_m being the fading coefficient. The probability density function (PDF) and the cumulative distribution function (CDF) of g_m are given, respectively, as

$$f_{g_m}(x) = \lambda_m \exp(-\lambda_m x), \tag{14}$$
$$F_{g_m}(x) = 1 - \exp(-\lambda_m x). \tag{15}$$

As mentioned earlier in the paper, in our analysis, the kth nearest SU to PU-Tx will be selected to forward the messages. This is performed by measuring the Euclidean distance from PU-Tx to each of the SUs. The PDF of the path loss d^{PL} for the kth nearest SU is distributed as [35]

$$f_{d^{PL}}(x) = \exp(-A_e x^\delta)\frac{\delta A_e^k x^{\delta k-1}}{\Gamma(k)}, \tag{16}$$

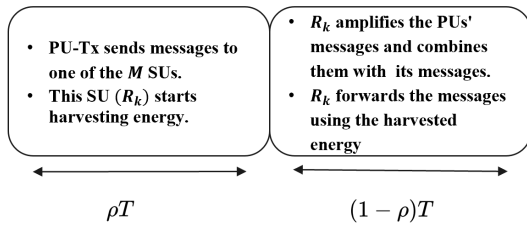where $A_e = \pi\phi$ and $\delta = \frac{U}{PL}$.

FIGURE 2. Frame structure of TS-based SWIPT in the proposed cognitive radio network.

III. OUTAGE PROBABILITY

The outage probability (OP) is defined as the probability that the data rate is lower than a predetermined rate threshold (R_{thi}), for $i = \{p, s\}$. Given this, R_{thp} represents the threshold for the PUs' link, whereas R_{ths} denotes the rate threshold for the SUs' communication. The outage probability is given by

$$OP = \mathbb{P}(R_j \le R_{thi}), \tag{17}$$

where $\mathbb{P}(\cdot)$ denotes the probability operator and $j \in (P, S)$. In this section, the outage probability for the PUs and SUs links is evaluated to reveal the reliability of the considered communication system.

A. OUTAGE PROBABILITY OF THE PRIMARY USERS' NETWORK

Considering the outage probability to assess the PUs communication quality is significant since the PUs receive their own messages in addition to the SUs messages, which are regarded as interference. The outage probability for the PUs' link is evaluated in this section by rewriting (17) using (12) and (8) as

$$OP = \mathbb{P}(a g_{RD} g_{SR} \le bJ g_{RD} d^{PL} + Jc g_{RD} g_{SR} + N_0 J d^{PL})$$
$$= \mathbb{P}\left(g_{SR} \le \frac{bJ}{a - Jc} d^{PL} + \frac{N_0 J}{(a - Jc)} L\right)$$
$$= \int_0^\infty \int_0^\infty F_{g_{SR}}(c_1 z + c_2 l) f_{d^{PL}}(z) f_L(l) \, dz \, dl, \tag{18}$$

where $J = 2^{\frac{R_{thp}}{(1-\rho)T}} - 1$, $c_1 = \frac{bJ}{a - Jc}$, $c_2 = \frac{N_0 J}{a - Jc}$, and $L = \frac{d^{PL}}{g_{RD}}$. First, one needs to obtain the PDF of the variable L as

$$f_L(x) = \int_0^\infty y f_{d^{PL}}(xy) f_{g_{RD}}(y) \, dy. \tag{19}$$

Substituting (16) and (14) into (19) for $m = RD$ yields

$$f_L(x) = \frac{\delta A_e^k \lambda_{RD}}{\Gamma(k)} x^{\delta k - 1} \int_0^\infty y^{\delta k} G_{0\,1}^{1\,0} \left({}_0^- \big| \lambda_{RD} y \right)$$
$$\times G_{0\,1}^{1\,0} \left({}_0^- \big| A_e x^\delta y^\delta \right) dy, \tag{20}$$

where $G_{p\,q}^{m\,n} \left({}_{b_s}^{a_r} \big| z \right)$ is the Meijer G-function defined in [36, Eq. 9-301]. Using [37, eq. (2.24.1.1)], the PDF of L is found as

$$f_L(x) = c_3 x^{\delta k - 1} G_{\delta\,1}^{1\,\delta} \left({}_0^{-k} \bigg| \frac{A_e x^\delta \delta^\delta}{\lambda_{RD}^\delta} \right), \tag{21}$$

where $c_3 = \frac{\delta^{1.5 + \delta k} A_e^k \lambda_{RD}^{-\delta k}}{\Gamma(k)(2\pi)^{(\delta - 1)0.5}}$. The outage probability of the PUs' link given in (18) is expressed as

$$OP = \frac{c_3 \delta A_e^k}{\Gamma(k)} \int_0^\infty \int_0^\infty \left[1 - \exp^{-\lambda_{SR}(c_1 z + c_2 l)} \right]$$
$$\times \exp\left(-A_e z^\delta\right) z^{\delta k - 1} l^{\delta k - 1} G_{\delta\,1}^{1\,\delta} \left({}_0^{-k} \bigg| \frac{A_e l^\delta \delta^\delta}{\lambda_{RD}^\delta} \right) dz \, dl$$
$$= 1 - \frac{c_3 \delta A_e^k}{\Gamma(k)} I_1 I_2, \tag{22}$$

where I_1 and I_2 are respectively given by

$$I_1 = \int_{z=0}^\infty z^{\delta k - 1} G_{0\,1}^{1\,0} \left({}_0^- \big| \lambda_{SR} c_1 z \right) G_{0\,1}^{1\,0} \left({}_0^- \big| A_e z^\delta \right) dz, \tag{23}$$

$$I_2 = \int_{l=0}^\infty l^{\delta k - 1} G_{0\,1}^{1\,0} \left({}_0^- \big| \lambda_{SR} c_2 l \right) G_{\delta\,1}^{1\,\delta} \left({}_0^{-k} \bigg| \frac{A_e \delta^\delta l^\delta}{\lambda_{RD}^\delta} \right) dl. \tag{24}$$

Using [37, eq.(2.24.1.1)], I_1 and I_2 are respectively solved as

$$I_1 = \frac{\delta^{\delta k - 0.5}}{(2\pi)^{(\delta - 1)0.5}(c_1 \lambda_{SR})^{\delta k}} G_{\delta\,1}^{1\,\delta} \left({}_{0}^{\Delta(\delta, 1 - \delta k)} \bigg| \frac{A_e \delta^\delta}{(\lambda_{SR} c_1)^\delta} \right), \tag{25}$$

$$I_2 = \frac{\delta^{\delta k - 0.5}}{(2\pi)^{(\delta - 1)0.5}(c_2 \lambda_{SR})^{\delta k}}$$
$$\times G_{2\delta\,1}^{1\,2\delta} \left({}_{0}^{-k, \Delta(\delta, 1 - \delta k)} \bigg| \frac{A_e \delta^{2\delta}}{(\lambda_{SR} \lambda_{RD} c_2)^\delta} \right), \tag{26}$$

where $\Delta(\delta, 1 - \delta k) = \frac{1 - \delta k}{\delta}, \frac{2 - \delta k}{\delta}, \cdots, \frac{\delta - \delta k}{\delta}$.

-Asymptotic Outage probability of the PUs' Link:

Herein, the asymptotic OP for the PUs' link is evaluated as the PU transmission power takes very high values. First, one must rewrite I_1 in (25) as

$$I_1 = \frac{D}{A^k} G_{\delta\,1}^{1\,\delta} \left({}_{k}^{\Delta(\delta, 1 - \delta k)} \big| A P_s^\delta \right), \tag{27}$$

where $D = \frac{\delta^{\delta k - 0.5}}{(2\pi)^{(\delta - 1)0.5} l_1^{\delta k}}$, $A = \frac{A_e \delta^\delta}{(\lambda_{SR} l_1)^\delta}$, and $l_1 = \frac{bJ \lambda_{SR}^{-\delta k}}{\frac{\alpha \rho \eta}{1 - \rho} - J \frac{(1 - \alpha)\rho \eta}{1 - \rho}}$. Transforming (27) into its integral form yields

$$I_1 = \frac{D}{A^k} \int_C \Gamma(k - s) \Gamma\left(1 - \frac{1}{\delta} + s\right) \Gamma\left(1 - \frac{2}{\delta} + s\right) \cdots$$
$$\times \Gamma(s) A^s P_s^{\delta s} ds. \tag{28}$$

It is seen that as $P_s \to \infty$, $I_1 \to \infty$. Hence, the asymptotic expression of I_1 is evaluated using the residue method defined in [38] as

$$I_1^{Asymp} \approx \frac{D}{A^k} \Gamma(k) \Gamma\left(1 - \frac{1}{\delta}\right) \Gamma\left(1 - \frac{2}{\delta}\right). \tag{29}$$

Similarly, I_2 is approximated as

$$I_2^{Asymp} \approx \frac{B}{L^k} \Gamma(k) \Gamma\left(1 - \frac{1}{\delta}\right) \Gamma\left(1 - \frac{2}{\delta}\right), \tag{30}$$

where $B = \frac{\delta^{\delta k - 0.5}}{(2\pi)^{(\delta-1)0.5} l_2^{\delta k}}$, $W = \frac{A_e \delta^{2\delta}}{(\lambda_{SR} \lambda_{RD} l_2)^\delta}$, and $l_2 = \frac{N_0 J}{\frac{\alpha \rho \eta}{1-\rho} - J \frac{(1-\alpha)\rho \eta}{1-\rho}}$. Given (37) and (38), OP is finally approximated as

$$OP_P^{Asymp} \approx 1 - \frac{c_3 \delta A_e^k}{\Gamma(k)} I_1^{Asymp} I_2^{Asymp}. \tag{31}$$

It is evident from (31) that the asymptotic outage probability is independent of P_s. This demonstrates that once the PU transmission power exceeds a certain level, there is no advantage to increasing it further. This is because the system no longer benefits from the power's impact on the system reliability. This result will be further clarified and investigated in the numerical results section.

B. OUTAGE PROBABILITY OF THE SECONDARY USERS' COMMUNICATION

Given the fact that the SU receiver also receives PUs messages that are superimposed with its own, it is critical to assess the SUs link's outage probability. The outage probability of the SUs link is evaluated using (17), which is expressed in terms of (11) and (13) as

$$OP = \mathbb{P}\left(g_{SR} \leq d_1 \frac{d^{PL}}{g_{RE}} + d_2 d^{PL}\right), \tag{32}$$

where $d_1 = \frac{\epsilon N_o}{q - \epsilon w}$, $d_2 = \frac{\epsilon e}{q - \epsilon w}$, and $\epsilon = 2^{\frac{R_{ths}}{(1-\rho)T}} - 1$. Following the same procedure to find (22), the OP of the SUs' link is expressed as

$$OP = 1 - \frac{d_3 \delta A_e^k}{\Gamma(k)} H_1 H_2, \tag{33}$$

where $d_3 = \frac{\delta^{1.5 + \delta k} A_e^k \lambda_{RE}^{-\delta k}}{\Gamma(k)(2\pi)^{(\delta-1)0.5}}$. Following the same procedure utilized to derive I_1 and I_2, H_1 and H_2 are found, respectively as

$$H_1 = \frac{\delta^{\delta k - 0.5}}{(2\pi)^{(\delta-1)0.5} (d_2 \lambda_{SR})^{\delta k}}$$
$$\times G_{\delta\ 1}^{1\ \delta}\left(\Delta(\delta, 1 - \delta k) \ \Big| \ \frac{A_e \delta^\delta}{(\lambda_{SR} d_2)^\delta}\right), \tag{34}$$

$$H_2 = \frac{\delta^{\delta k - 0.5}}{(2\pi)^{(\delta-1)0.5} (d_1 \lambda_{SR})^{\delta k}}$$
$$\times G_{2\delta\ 1}^{1\ 2\delta}\left(-k, \Delta(\delta, 1 - \delta k) \ \Big| \ \frac{A_e \delta^{2\delta}}{(\lambda_{SR} \lambda_{RE} d_1)^\delta}\right). \tag{35}$$

-Asymptotic Outage probability of the SUs Link:
We evaluate the outage probability of the SUs link as the transmission power of the PU transmitter is asymptotically large, i.e., as $P_s \to \infty$. This is performed to observe the effect of the PUs transmission power on the received SUs messages' quality. Setting $P_s \to \infty$ and performing the approach to find the asymptotic OP for the PUs' link, the OP for the SUs' link is approximated as

$$OP_S^{Asymp} \approx 1 - \frac{d_3 \delta A_e^k}{\Gamma(k)} H_1^{Asymp} H_2^{Asymp}, \tag{36}$$

where H_1^{Asymp} is given as

$$H_1^{Asymp} \approx \frac{D'}{A'^k} \Gamma(k) \Gamma\left(1 - \frac{1}{\delta}\right) \Gamma\left(1 - \frac{2}{\delta}\right), \tag{37}$$

with $D' = \frac{\delta^{\delta k - 0.5}}{(2\pi)^{(\delta-1)b^*} l_1'^{\delta k}}$, $A = \frac{A_e \delta^\delta}{(\lambda_{SR} l_1')^\delta}$, and $l_1' = \frac{e \epsilon \lambda_{SR}^{-\delta k}}{\frac{(1-\alpha)\rho \eta}{1-\rho} - \epsilon \frac{\alpha \rho \eta}{1-\rho}}$. Moreover, H_2^{Asymp} is expressed as

$$H_2^{Asymp} \approx \frac{B'}{L'^k} \Gamma(k) \Gamma\left(1 - \frac{1}{\delta}\right) \Gamma\left(1 - \frac{2}{\delta}\right). \tag{38}$$

with $B' = \frac{\delta^{\delta k - 0.5}}{(2\pi)^{(\delta-1)0.5} l_2'^{\delta k}}$, $W' = \frac{A_e \delta^{2\delta}}{(\lambda_{SR} \lambda_{RE} l_2')^\delta}$, and $l_2' = \frac{N_0 \epsilon}{\frac{(1-\alpha)\rho \eta}{1-\rho} - \epsilon \frac{\alpha \rho \eta}{1-\rho}}$.

As seen from (36), when the PU transmission power is very large, the outage probability of the SUs link becomes independent of this power. This illustrates that the outage probability reaches its lowest level as P_s takes very high values. This effect will be investigated in the numerical results section.

IV. OPTIMIZATION PROBLEMS

Given that increasing the data rate reduces the probability of an outage, the primary goal of this section is to improve the networks' data rate in two distinct scenarios. We begin by optimizing the time switching factor (ρ) and the power allocation factor (α) that maximize the data rate of the SUs link while respecting the PUs' rate constraint. Following that, we optimize the same parameters that maximize the sum rate ($R_S + R_P$) to enhance the reliability of both networks. It is worth noting that by optimizing ρ, one may manage the time slots dedicated to energy harvesting and the time allocated to amplifying the user's messages via the AF protocol. Furthermore, optimizing α enables the evaluation of the amount of power required to transfer the messages of each network, and hence the amount of interference affecting each network.

A. MAXIMIZING THE SECONDARY USERS DATA RATE

In this section, the time switching factor (ρ) and the power allocation factor of R_k (α) are optimized with an objective of maximizing the SUs' rate while ensuring that the PUs' rate is maintained above a certain threshold (R_{pt}). This demonstrates that the SUs link's reliability may be improved while ensuring that the PUs' reception quality standards are met. Given this, the optimization problem is formulated as

$$\mathcal{P}1: \max_{\rho, \alpha} R_S \tag{39}$$
$$\text{s.t.} \quad 0 < \rho < 1, \tag{40}$$
$$0 < \alpha < 1, \tag{41}$$
$$R_P \geq R_{pt}. \tag{42}$$

This problem is clearly a non-convex one since it is a non-linear mixed-integer optimization problem, and hence, it is hard to be solved directly. Instead, it can be shown that it is a biconvex problem in ρ and α. As the term suggests, a biconvex problem is the one that is convex in α for a given

TABLE 1. Algorithm of solving a biconvex optimization problem.

Step 1	Assume G demonstrates the biconvex set of α and ρ and select an arbitrary initial point for these parameters, i.e., (α_0, ρ_0).
Step 2	For a fixed value of ρ, find the optimal value of α (α^*) for the convex problem using the Lagrangian dual method through the method of the gradient decent.
Step 3	Using α^*, search for the optimal value of ρ (ρ^*) for the convex problem using the Lagrangian dual method.
Step 4	Once the maximum R_s is obtained through the substitution of α^* and ρ^*, the process is terminated.

value of ρ, and convex in ρ for a fixed α. This can be easily shown by several methods, such as plotting the functions on Matlab. Similar to [24], this type of problem can be solved using the algorithm described in Table 1. As mentioned in the table, one can use the Lagrangian approach to find the optimal value of ρ and α. The Lagrangian of $\mathcal{P}1$ can be expressed as

$$\mathcal{L}(\zeta, \xi_1, \xi_2, \xi_3) = R_S + \xi_1(\zeta - 1) + \xi_2(-\zeta)$$
$$+ \xi_3(R_{pt} - R_P), \quad (43)$$

where $\xi_1, \xi_2,$ and ξ_3 represent the dual variables associated with the constraint on ζ, for $\zeta \in (\rho, \alpha)$, and the PUs' rate in (42), respectively. Then, the Lagrange dual function of $\mathcal{P}1$ is expressed as

$$\mathcal{L}(\xi_1, \xi_2, \xi_3) = \max_{\zeta} \mathcal{L}(\zeta; \xi_1, \xi_2, \xi_3). \quad (44)$$

Using the partial derivative and the method of the gradient descent, the values of $\rho^*, \alpha^*, \xi_1, \xi_2,$ and ξ_3 are found.

B. MAXIMIZING THE SUM RATE
In this section, the time switching factor and the power allocation factor which maximize the sum rate ($R_S + R_P$) are evaluated. Optimizing the sum rate has the potential to increase the reliability of both networks by lowering their outage probability. This optimization problem is formulated as

$$\mathcal{P}2: \max_{\rho, \alpha} R_P + R_S \quad (45)$$
$$\text{s.t.} \quad 0 < \rho < 1, \quad (46)$$
$$0 < \alpha < 1. \quad (47)$$

The sum rate is a biconvex function and thus this problem can be solved using the methodology described in Table 1.

V. NUMERICAL RESULTS
In this section, our theoretical analyses and Monte-Carlo simulations are presented. Assume a two-dimensional (2D) area ($U = 2$) and a HPPP distribution of the relays locations. 10^5 realizations of the positions of the relays are generated in a square area of a side of 20 meters (m). Moreover, to take the distance between the nodes into account, we let $d_{xy}^{-PL} = \frac{1}{2\lambda_{xy}}$, in which d_{xy} is the distance between nodes x and y, with $xy = \{SR, RD, RE\}$.

Figure 3 presents the outage probability of the PUs' link versus the density of SUs. It is observed that when the number of SUs increases in the network, the reliability of the PUs
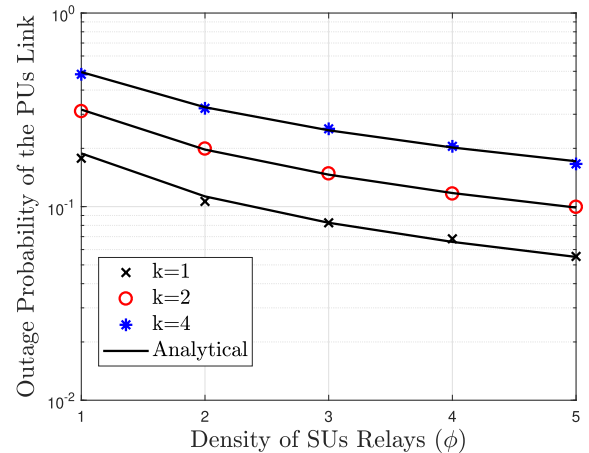

FIGURE 3. Outage probability of the PUs link versus the density of the SUs relay for different values of k. $\rho = 0.5$, $PL = 2$, $\lambda_{RD} = 0.5$, $\lambda_{SR} = 0.5$, $T = 1$, $R_{thp} = 0.5$, $P_s = 5$ dB, $\alpha = 0.8$, $N_0 = 1$, and $\eta = 0.8$.

transmission improves. This is owing to the fact that the more densely populated the area is with SUs, the more likely it is to have an SU closer to the PU transmitter with superior channel characteristics. Moreover, in contrast to the fourth nearest user ($k = 4$), selecting the first closest SU to the PU transmitter, i.e., $k = 1$, has the greatest impact on improving the performance of the PUs' communication. That is, there is a larger probability that the closest user will be able to effectively deliver the PUs messages. However, in certain scenarios, the fourth nearest SU can be used to forward the PUs' messages in an instance wherein the first nearest, second nearest, and the third nearest SUs are no longer available for transmission. This demonstrates the critical role of assuming several relays with randomly assigned locations.

Figure 4 illustrates the outage probability of the PUs' communication against the time switching factor (ρ). It is observed that the outage probability is a convex function of ρ. As ρ increases, demonstrating more time is allocated for harvesting energy, a higher SNR is achieved at the PU receiver and consequently a better system performance. However, beyond the minimum value of ρ, the system's reliability worsens. This depicts the scenario in which the time slot left for amplifying the PUs messages and forwarding them to the destination $(1 - \rho)$ is small. Additionally, as the energy harvesting efficiency coefficient (η) increases, the outage probability reduces. This is because a greater η indicates that the relaying SU is capable of harvesting more energy, implying that more power is available for messages' delivery.

Figure 5 reflects the impact of the SUs transmission on the PUs' communication. As mentioned earlier in this paper, the PU receiver regards the SUs messages as interference. Hence, as $(1 - \alpha)$ increases, which is the portion of SU relay's power dedicated to forwarding SUs messages, the PUs communication becomes more susceptible to outages. In addition, this figure depicts the effect of the fading severity level of the h_{RD} channel on the PUs' communication, as represented by λ_{RD}. It is found that when λ_{RD} increases, the fading becomes more severe, resulting in a poor reception at the PU destination.
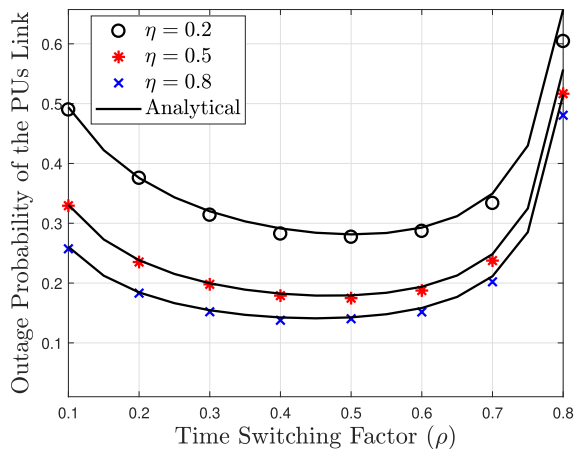
FIGURE 4. Outage probability of the PUs link versus the time switching factor for different values of η. $k = 1$, $PL = 2$, $\lambda_{RD} = 0.5$, $\lambda_{SR} = 0.5$, $T = 1$, $R_{thp} = 0.4$, $PL = 2$, $P_S = 5$ dB, $\alpha = 0.8$, $N_0 = 1$, and $\phi = 1$.
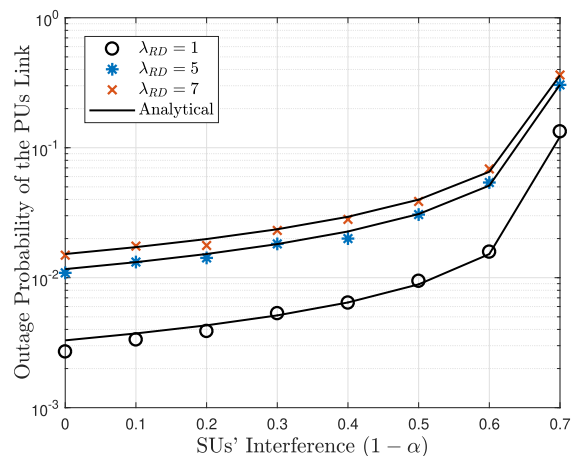

FIGURE 5. Outage probability of the PUs link versus the interference caused by the SUs transmissions. $k = 1$, $\delta = 1$, $\lambda_{SR} = 1$, $T = 1$, $R_{thp} = 0.2$, $P_S = 5$ dB, $\eta = 0.7$, $\rho = 0.6$, $N_0 = 1$, $\phi = 100$, and $k = 1$.

FIGURE 6. Outage probability of PUs' and SUs' links versus SUs density. $k = 1$, $PL = 2$, $\lambda_{SR} = 1$, $\lambda_{RD} = 1$, $\lambda_{RE} = 1$, $T = 1$, $R_{thp} = 0.1$, $R_{ths} = 0.1$, $P_S = 5$ dB, $\rho = 0.6$, $\eta = 0.7$, $N_0 = 1$ and $k = 1$.

FIGURE 7. Outage probability versus α. $k = 1$, $\rho = 0.5$, $\eta = 0.2$, $\lambda_{RD} = 0.5$, $PL = 2$, $\lambda_{SR} = 0.5$, $T = 1$, $R_{thp} = 0.2$, $R_{ths} = 0.2$, $P_S = 2$ dB, $\phi = 5$. $d_{SR} = 0.5$ m, $d_{RD} = 0.5$ m, $d_{RE} = 0.5$ m, $N_0 = 1$, and $d_{SP(direct)} = 1m$.

Figure 6 depicts the impact of the PUs transmissions on the quality of the SUs' communication. As the proportion of the relay's power dedicated to PU transmission (α) increases, the probability of an outage in the SUs' communication increases. This is because as α rises, the SU receiver becomes more subject to the interference caused by the PUs transmissions. Additionally, as α increases, the portion of power assigned to the SUs' communication at the relay decreases, raising the probability of a SUs' transmission outage. However, a higher α suggests that a greater amount of the power is assigned to convey the PUs messages, resulting in a lower PUs' link outage probability. Finally, since the same relay that forwards PUs' messages also forwards SUs' messages, as the density of the SUs relays increases, the reliability of the SUs network improves.

Figure 7 reveals the significance of sharing in overlay CRN. In this figure, we compare the overlay CRN with direct transmission, in which we presume that the PUs can communicate directly without the assistance of SUs. As shown in the figure, when α is between 0.35 and 0.65, the overlay CRN outperforms the direct transmission since the attained
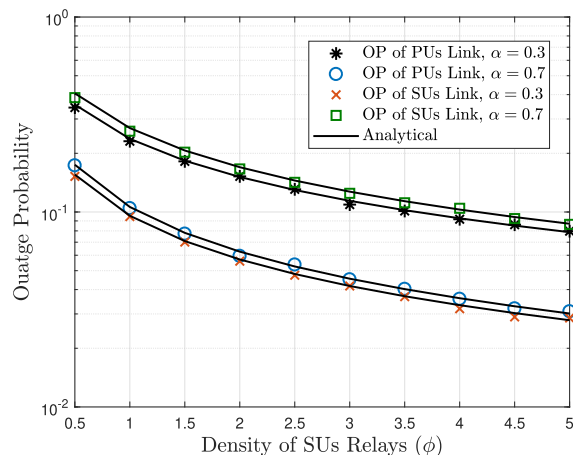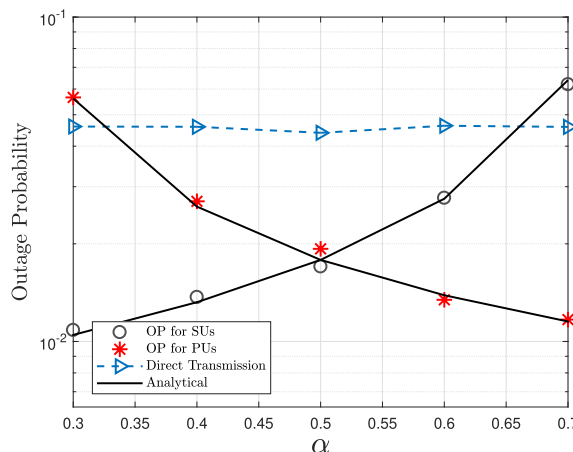
outage probability is lower. This applies to both SUs and PUs networks. Moreover, it is evident that when $\alpha = 0.5$, both networks function similarly. In addition, when $\alpha < 0.5$, the SUs' communication reliability is greater than the PUs', however, when $\alpha > 0.5$, the PUs' reliability steadily improves to surpass the SUs'. This illustrates the importance of optimizing α to be able to decide how to distribute the power of the SU relay and control the interference caused by one network on another.

Figure 8 shows the outage probability of the SUs network versus the transmission power of the PU-Tx (P_s). It can be seen that as P_s increases, the outage probability decreases. This is because as P_s increases, the amount of energy harvested at the SU relay increases, leading to improved SUs' link reliability. In addition, the figure shows the asymptotic outage probability of the SUs' link, which represents the scenario when P_s approaches ∞. It is obvious that as P_s reaches this value, the system is in optimal condition. This is due to the fact that the harvested energy will be high, and thus the received SINR will be improved, resulting in a zero outage
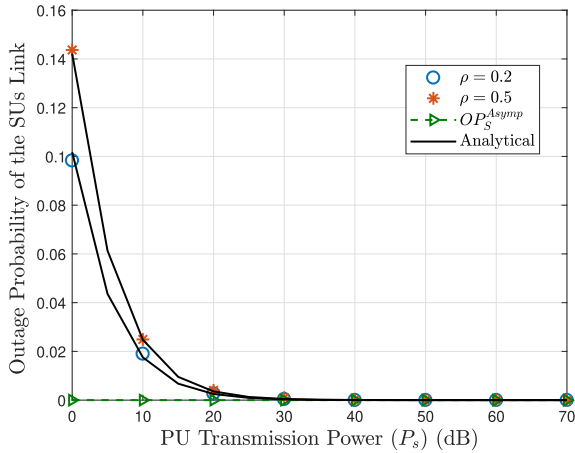
FIGURE 8. Outage probability of the SUs versus P_s. $k = 1$, $\eta = 0.2$, $\lambda_{RE} = 0.5$, $\lambda_{SR} = 0.1$, $T = 1$, $R_{ths} = 1$, $PL = 2$, $\alpha = 0.2$, $N_0 = 1$, and $\phi = 5$.
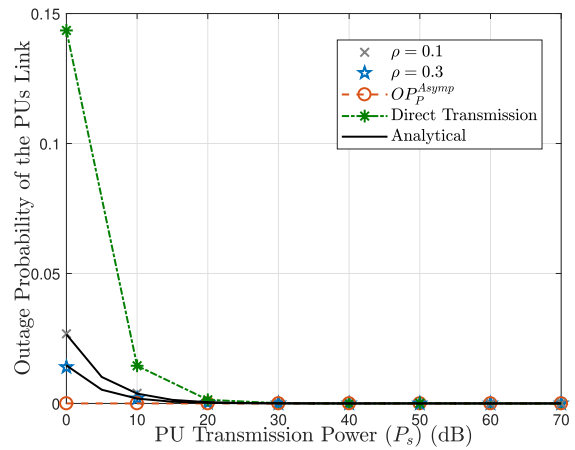

FIGURE 9. Outage probability of the PUs versus P_s. $k = 1$, $PL = 2$, $\eta = 0.9$, $d_{SR} = 0.5 \, m$, $d_{RD} = 0.5 \, m$, $T = 1$, $R_{thp} = 0.4$, $\alpha = 0.8$, $N_0 = 1$, and $\phi = 5$.

FIGURE 10. SUs' rate link versus P_s. $k = 1$, $\eta = 0.8$, $\lambda_{RD} = 1$, $\lambda_{SR} = 0.5$, $\lambda_{RE} = 1$, $T = 1$, $R_{pt} = 0.5$, $N_0 = 1$, and $\phi = 1$.

FIGURE 11. SUs' rate link versus P_s. $k = 1$, $\eta = 0.8$, $\lambda_{RD} = 1$, $\lambda_{SR} = 0.5$, $\lambda_{RE} = 1$, $T = 1$, $R_{pt} = 0.1$, $N_0 = 1$, and $\phi = 1$.

probability. Moreover, one can notice that the outage probability agrees with the asymptotic one at high values of P_s.

Figure 9 illustrates the outage probability for the PUs link versus the PU transmission power P_s. As P_s increases, the PUs' communication quality improves. This is attributed to the fact that boosting the PU-Tx transmission power increases the harvested energy at the assistant SU. As the amount of energy gathered increases, the amplification factor increases, resulting in a higher reception quality at PU-Rx. In addition, the saturation that occurs at high P_s indicates that boosting the power has no benefit after a particular level of P_s. This is owing to the belief that as P_s becomes very large, the outage probability becomes independent of this power and reaches its optimum situation, i.e. $OP \approx 0$. This is also confirmed by the agreement between the outage probability at high P_s and the asymptotic outage probability obtained in (36) as $P_s \rightarrow \infty$. Furthermore, despite the independence on P_s, the results demonstrate that the overlay CRN outperforms the direct transmission between PUs, i.e., without the assistance of SUs.

When P_s is very high, the relay harvests a high energy and this will reach us to the best system performance, in which the OP approaches zero. In this case, the system i also indepen-
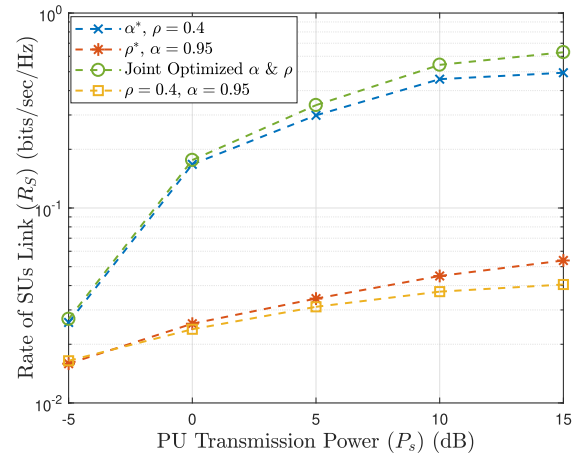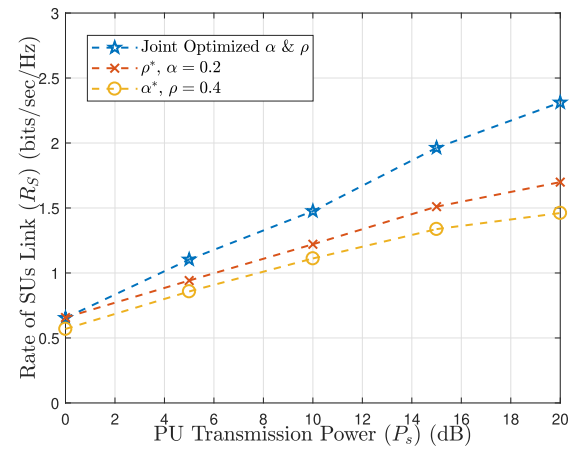
dent of P_R, which means that is the PU-Tx is able to increase its transmission power to a very high value without impact other PUs, no need for sharing. This also means that after a certain value of P_s, no need to increase it to make the outage decrease as it saturates. The OP for the direct transmission is still the worst, which means that the overlay CRN still outperforms the direct.

Figure 10 depicts the SUs' link rate versus the transmission power of the PU-Tx (P_s). By comparing the fixed value of ρ and α with the optimum ones (ρ^*, α^*), it is clear that the SUs achieve the optimum link rate when ρ and α are chosen according to the optimization problem in (39). In addition, the results indicate the benefit of performing a joint optimization for both parameters rather than optimizing a single parameter ((α^*, $\rho = 0.4$) and (ρ^*, $\alpha = 0.95$)). Particularly, the SUs achieve the highest rate when both parameters are optimized jointly. This highlights the significant importance of having an adjustable time switching factor and power allocation factor in the EH process. An optimized α assists in determining the amount of SU relay power that should be used for each network while controlling the interference caused by one network on another. Moreover, by optimizing ρ, one can
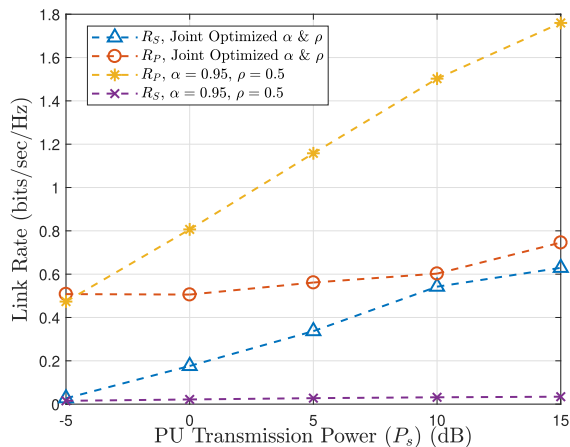
FIGURE 12. SUs' and PUs' link rate versus P_s. $k = 1$, $\eta = 0.8$, $PL = 2$, $\lambda_{RE} = 1$, $\lambda_{RD} = 1$, $\lambda_{SR} = 0.5$, $N_0 = 1$, $T = 1$, $R_{pt} = 0.5$, and $\phi = 1$.
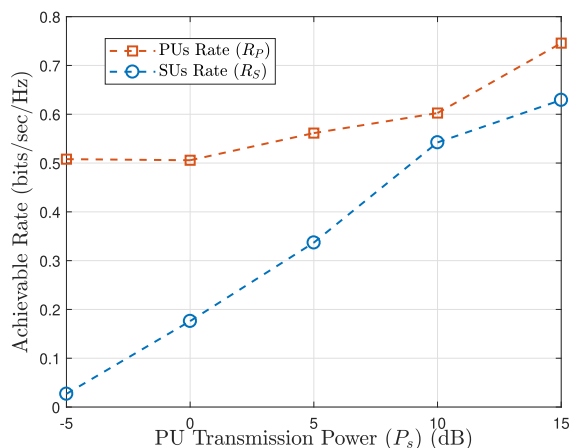

FIGURE 14. Outage probability of the SUs link versus the threshold rate of the PUs' link R_{pt}. $k = 1$, $\eta = 0.8$, $\lambda_{RD} = 1$, $\lambda_{SR} = 0.5$, $\lambda_{RE} = 0.5$, $T = 1$, $P_S = 15$ dB, $\rho = 0.4$, and $\phi = 1$.

FIGURE 13. SUs' and PUs' link rate versus P_S for joint optimized ρ and α. $k = 1$, $\eta = 0.8$, $PL = 2$, $\lambda_{RE} = 1$, $\lambda_{RD} = 1$, $\lambda_{SR} = 0.5$, $T = 1$, $R_{pt} = 0.5$, $N_0 = 1$, and $\phi = 1$.

FIGURE 15. Sum rate versus P_S for different values of α and ρ. $k = 1$, $\eta = 0.8$, $\lambda_{RD} = 1$, $\lambda_{SR} = 0.5$, $\lambda_{RE} = 1$, $T = 1$, and $\phi = 1$.

determine the time slots assigned for the EH process and the amplifying and forwarding process. Furthermore, it is noticed that optimizing both parameters yields a result that is closer to optimizing α independently for fixed ρ. This depends on the selected values of the fixed parameters and the PUs rate threshold. To illustrate a scenario in which the joint optimization approach gets close to optimizing solely ρ, the threshold in Figure 11 is considered to be lower than the one in Figure 10 with different fixed values chosen for the single optimization scenarios. The figure indicates that when optimizing ρ, selecting lower α and R_{pt} results in rising the impact of optimizing ρ, as it gets closer to the joint optimization. Additionally, it is worth mentioning that the fixed values of ρ and α selected from the feasibility region of problem $\mathcal{P}1$.

Figure 12 presents the links rates of the SUs and PUs communication against P_s. It is observed that optimizing the parameters α and ρ improves the SUs rate. Moreover, even with fixed parameters, i.e. without optimization, the PUs' rate remains greater than the threshold rate (R_{pt}). This ensures that the performance of the PUs' link is preserved above the minimum allowed level. In addition, whether the parameters
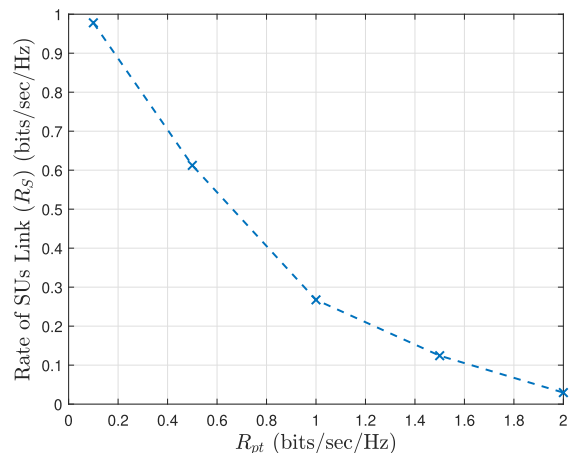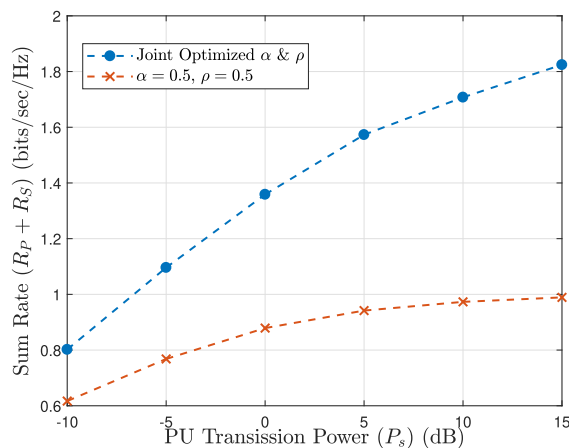
are optimized or fixed, the PUs' rate remains greater than the SUs' rate. Additionally, Figure 13 shows both rates against P_s when α and ρ are optimized. It is concluded that regardless of the transmission power level of PU-Tx, the PUs' rate is maintained above the threshold ($R_P \geq 0.5$).

Figure 14 depicts the rate of the secondary users versus the threshold of the PUs rate constraint (R_{pt}) defined in the optimization problem ($\mathcal{P}1$) assuming fixed ρ. This is to clearly show the impact of this threshold on the optimization process. As R_{pt} increases, the SUs' communication reliability degrades. This is because a higher threshold rate for the PU's communication involves altering α to maximize not only the SU's rate but also maintaining the PU's rate above this threshold. Despite the fact this constraint is not to the greatest advantage of the SUs' transmission, this ensures that the PUs' communication reliability remains within acceptable limits.

Finally, Figure 15 presents the sum-rate of both networks versus the PU transmission power (P_s). It is observed that using the time switching factor and the power allocation factor optimized in problem $\mathcal{P}2$ (ρ^* and α^*) provides the best performance when compared to fixed ρ and α. Notably, optimizing the sum rate has the advantage of

simultaneously enhancing both networks' reliability, regardless of the interference imposed by one network on the other. As a result, all users in this cooperating CRN will have stable communication.

VI. CONCLUSION

This paper investigates an overlay cognitive radio network with two primary users (PUs) and several randomly distributed secondary users (SUs). In exchange for accessing the licensed band, one of these multiple SUs is selected to forward the PUs messages using the harvested energy from the PU transmitter messages. Our results indicate that a larger density of these SUs is necessary to boost the link reliability of the PUs and SUs communication in terms of outage probability. We have derived the outage probability of both links and their asymptotic expressions, and our results demonstrate that the system approaches zero outage probability with high PU transmission power. In addition, the effectiveness of overlay CRN was shown by comparing the overlay access mode to direct transmission, indicating that the overlay mode outperforms the direct transmission over a certain range of the power allocation factor (α). In addition, the time switching factor (ρ) and α are optimized for two scenarios: maximizing the SUs' rate while constraining the PUs' rate, and maximizing the sum of both networks' rates. In this work, we highlight the importance of optimizing ρ, since this parameter dictates the optimal harvesting time relative to the forwarding time. In addition, optimizing α in our research revealed the amount of power that the selected relay should use for SU transmissions and that for PU transmissions, therefore limiting the amount of interference imposed on each network. Our results demonstrate that, as compared to fixed factors, the derived optimized ones achieve the optimum performance. In addition, our findings evaluate the effect of EH in minimizing the probability of network outages for PUs. In other words, as the energy harvesting efficiency coefficient (η) rises, more energy is harvested at the relay, and as a result, there is more power available for message delivery. Finally, the agreement between the analytical and Monte-Carlo simulations demonstrates the validity of our mathematical computations and the capability of applying the analyses and system model to energy-constrained devices, such as cognitive wireless sensor networks.

Incorporating machine learning (ML) strategies for relay selection might be a potential future avenue of investigation. An ML technique might be used to select the SU relay that maximizes energy efficiency and reduces outage probability for PUs and SUs' networks. This will boost the performance of the networks with low complexity.

REFERENCES

[1] N. A. Khalek and W. Hamouda, "Learning-based cooperative spectrum sensing in hybrid underlay-interweave secondary networks," in *Proc. IEEE Global Commun. Conf. (GLOBECOM)*, Dec. 2020, pp. 1–6.

[2] N. A. Khalek and W. Hamouda, "Intelligent spectrum sensing: An unsupervised learning approach based on dimensionality reduction," in *Proc. IEEE Int. Conf. Commun. (ICC)*, May 2022, pp. 171–176.

[3] A. Goldsmith, S. A. Jafar, I. Maric, and S. Srinivasa, "Breaking spectrum gridlock with cognitive radios: An information theoretic perspective," *Proc. IEEE*, vol. 97, no. 5, pp. 894–914, Apr. 2009.

[4] N. A. Khalek and W. Hamouda, "Unsupervised two-stage learning framework for cooperative spectrum sensing," in *Proc. IEEE Int. Conf. Commun. (ICC)*, Jun. 2021, pp. 1–6.

[5] D. H. Tashman and W. Hamouda, "Physical-layer security on maximal ratio combining for SIMO cognitive radio networks over cascaded κ-μ fading channels," *IEEE Trans. Cognit. Commun. Netw.*, vol. 7, no. 4, pp. 1244–1252, Dec. 2021.

[6] D. H. Tashman and W. Hamouda, "Physical-layer security for cognitive radio networks over cascaded Rayleigh fading channels," in *Proc. IEEE Global Commun. Conf. (GLOBECOM)*, Dec. 2020, pp. 1–6.

[7] N. A. Khalek and W. Hamouda, "From cognitive to intelligent secondary cooperative networks for the future internet: Design, advances, and challenges," *IEEE Netw.*, vol. 35, no. 3, pp. 168–175, May 2021.

[8] D. H. Tashman and W. Hamouda, "An overview and future directions on physical-layer security for cognitive radio networks," *IEEE Netw.*, vol. 35, no. 3, pp. 205–211, Oct. 2021.

[9] Y. Alsaba, S. K. A. Rahim, and C. Y. Leow, "Beamforming in wireless energy harvesting communications systems: A survey," *IEEE Commun. Surveys Tuts.*, vol. 20, no. 2, pp. 1329–1360, Jan. 2018.

[10] D. C. Melgarejo, J. M. Moualeu, P. Nardelli, G. Fraidenraich, and D. B. da Costa, "GFDM-based cooperative relaying networks with wireless energy harvesting," in *Proc. 16th Int. Symp. Wireless Commun. Syst. (ISWCS)*, Aug. 2019, pp. 416–421.

[11] T. D. P. Perera, D. N. K. Jayakody, S. K. Sharma, S. Chatzinotas, and J. Li, "Simultaneous wireless information and power transfer (SWIPT): Recent advances and future challenges," *IEEE Commun. Surveys Tuts.*, vol. 20, no. 1, pp. 264–302, Dec. 2018.

[12] D. H. Tashman and W. Hamouda, "Secrecy analysis for energy harvesting-enabled cognitive radio networks in cascaded fading channels," in *Proc. IEEE Int. Conf. Commun. (ICC)*, Jun. 2021, pp. 1–6.

[13] M.-L. Ku, W. Li, Y. Chen, and K. J. R. Liu, "Advances in energy harvesting communications: Past, present, and future challenges," *IEEE Commun. Surveys Tuts.*, vol. 18, no. 2, pp. 1384–1412, Nov. 2016.

[14] D. Tashman, W. A. Hamouda, and J. M. Moualeu, "On securing cognitive radio networks-enabled SWIPT over cascaded-fading channels with multiple eavesdroppers," *IEEE Trans. Veh. Technol.*, vol. 71, no. 1, pp. 478–488, Nov. 2021.

[15] Z. Yan, S. Chen, X. Zhang, and H. L. Liu, "Outage performance analysis of wireless energy harvesting relay-assisted random underlay cognitive networks," *IEEE Internet Things J.*, vol. 5, no. 4, pp. 2691–2699, Feb. 2018.

[16] X. Ding, Y. Zou, G. Zhang, X. Chen, X. Wang, and L. Hanzo, "The security–reliability tradeoff of multiuser scheduling-aided energy harvesting cognitive radio networks," *IEEE Trans. Commun.*, vol. 67, no. 6, pp. 3890–3904, Mar. 2019.

[17] Z. Ali, G. A. S. Sidhu, M. Waqas, L. Xing, and F. Gao, "A joint optimization framework for energy harvesting based cooperative CR networks," *IEEE Trans. Cognit. Commun. Netw.*, vol. 5, no. 2, pp. 452–462, Apr. 2019.

[18] J. Ye, Z. Liu, H. Zhao, G. Pan, Q. Ni, and M.-S. Alouini, "Relay selections for cooperative underlay CR systems with energy harvesting," *IEEE Trans. Cognit. Commun. Netw.*, vol. 5, no. 2, pp. 358–369, Apr. 2019.

[19] T. Mashiri, F. Takawira, and J. M. Moualeu, "Relay selection in massive MIMO wireless energy harvesting cognitive network," in *Proc. IEEE AFRICON*, Sep. 2019, pp. 1–5.

[20] D. H. Tashman and W. Hamouda, "Towards improving the security of cognitive radio networks-based energy harvesting," in *Proc. IEEE Int. Conf. Commun. (ICC)*, May 2022, pp. 3436–3441.

[21] M. H. Khoshafa, J. M. Moualeu, T. M. N. Ngatched, and M. H. Ahmed, "On the performance of secure underlay cognitive radio networks with energy harvesting and dual-antenna selection," *IEEE Commun. Lett.*, vol. 25, no. 6, pp. 1815–1819, Mar. 2021.

[22] D. H. Tashman and W. Hamouda, "Cascaded κ-μ fading channels with colluding eavesdroppers: Physical-layer security analysis," in *Proc. Int. Conf. Commun., Signal Process., Appl. (ICCSPA)*, Mar. 2021, pp. 1–6.

[23] D. H. Tashman, W. Hamouda, and I. Dayoub, "Secrecy analysis over cascaded κ-μ fading channels with multiple eavesdroppers," *IEEE Trans. Veh. Technol.*, vol. 69, no. 8, pp. 8433–8442, May 2020.

[24] Z. Wang, Z. Chen, B. Xia, L. Luo, and J. Zhou, "Cognitive relay networks with energy harvesting and information transfer: Design, analysis, and optimization," *IEEE Trans. Wireless Commun.*, vol. 15, no. 4, pp. 2562–2576, Dec. 2016.

[25] D. S. Gurjar, H. H. Nguyen, and H. D. Tuan, "Wireless information and power transfer for IoT applications in overlay cognitive radio networks," *IEEE Internet Things J.*, vol. 6, no. 2, pp. 3257–3270, Nov. 2019.

[26] K.-Y. Hsieh, F.-S. Tseng, M.-L. Ku, and C.-Y. Hsu, "Information and energy cooperation in overlay hierarchical cognitive radio networks," in *Proc. 10th Int. Conf. Ubiquitous Future Netw. (ICUFN)*, Jul. 2018, pp. 274–279.

[27] S. Solanki, P. K. Upadhyay, D. B. D. Costa, H. Ding, and J. M. Moualeu, "Performance analysis of piece-wise linear model of energy harvesting-based multiuser overlay spectrum sharing networks," *IEEE Open J. Commun. Soc.*, vol. 1, pp. 1820–1836, 2020.

[28] D. Xu and H. Zhu, "Sum-rate maximization of wireless powered primary users for cooperative CRNs: NOMA or TDMA at cognitive users?" *IEEE Trans. Commun.*, vol. 69, no. 7, pp. 4862–4876, Jul. 2021.

[29] D. Xu and Q. Li, "Cooperative resource allocation in cognitive radio networks with wireless powered primary users," *IEEE Wireless Commun. Lett.*, vol. 6, no. 5, pp. 658–661, Jul. 2017.

[30] D. Tashman, "Physical-layer security in cognitive radio networks," Ph.D. dissertation, Dept. Elect. Comput. Eng., Concordia Univ., Montreal, QC, Canada, 2022.

[31] D. Tashman and W. Hamouda, "Cascaded κ-μ fading channels with colluding and non-colluding eavesdroppers: Physical-layer security analysis," *Future Internet*, vol. 13, no. 8, p. 205, Aug. 2021.

[32] Z. Chen, B. Xia, and H. Liu, "Wireless information and power transfer in two-way amplify- and-forward relaying channels," in *Proc. IEEE Global Conf. Signal Inf. Process. (GlobalSIP)*, Dec. 2014, pp. 168–172.

[33] X. Shi, A. Huang, and T. Zhang, "Outage probability of two-way amplify-and-forward relaying over Nakagami-m fading channels," in *Proc. Int. Conf. Comput. Inf. Sci.*, Jun. 2013, pp. 1289–1292.

[34] X. Wang, H. Zhang, T. A. Gulliver, W. Shi, and H. Zhang, "Performance analysis of two-way AF cooperative relay networks over Weibull fading channels," *J. Commun.*, vol. 8, no. 6, pp. 372–377, Jun. 2013.

[35] M. Haenggi, "On distances in uniformly random networks," *IEEE Trans. Inf. Theory*, vol. 51, no. 10, pp. 3584–3586, Sep. 2005.

[36] I. S. Gradshteyn and I. M. Ryzhik, *Table of Integrals, Series, and Products*. New York, NY, USA: Academic, 2007.

[37] A. Prudnikov, Y. Brychkov, and O. Marichev, *Integrals and Series: More Special Functions*, vol. 3. New York, NY, USA: Gordon and Breach Science Publishers, 1990.

[38] H. Chergui, M. Benjillali, and S. Saoudi, "Performance analysis of project-and-forward relaying in mixed MIMO-pinhole and Rayleigh dual-hop channel," *IEEE Commun. Lett.*, vol. 20, no. 3, pp. 610–613, Mar. 2016.

in M2M and IoT communications and an IEEE Communications Society Distinguished Lecturer. His current research interests include single/multiuser multiple-input multiple-output communications, 5/6G technologies, massive MIMO, mm-wave communications, sensor networks, cognitive radios, the IoT, machine-to-machine communications, smart grid communications, and channel coding. He was a recipient of numerous awards, including the best paper awards of the GLOBECOM'2020, 2019 IEEE Conference on Communications, Signal Processing, and their Applications, IEEE WCNC'16, ICC 2009, and the IEEE Canada Certificate of Appreciation, in 2007 and 2008. He has been a Keynote Speaker of many conferences, including 13th IEEE International Conference on Computer Engineering and Systems (ICCES 2018), and Annual MSA Workshop on Advances in Communication and Electronics. He served(ing) as the Co-Chair of the IoT & Sensor Networks Symposium of the IEEE Globecom 2022, Wireless Communications and Networking Conference (WCNC, 2019) MAC and Cross-layer Design Track, and Wireless Communications Symposium of the IEEE ICC'2018, the Co-Chair of the Ad-hoc, Sensor, and Mesh Networking Symposium of the IEEE Globecom Conference 2017, the Technical Co-Chair of the Fifth International Conference on Selected Topics in Mobile and Wireless Networking (MoWNet'2016), the Track Co-Chair of the Multiple Antenna and Cooperative Communications and IEEE Vehicular Technology Conference (VTC-Fall'16), the Co-Chair of the ACM Performance Evaluation of Wireless Ad Hoc, Sensor, and Ubiquitous Networks (ACMPE WASUN'2014) 2014, and the Technical Co-Chair of the Wireless Networks Symposium, 2012 Global Communications Conference, the Ad-hoc, Sensor, and Mesh Networking Symposium of the 2010 ICC, and the 25th Queen's Biennial Symposium on Communications. He also served as the Track Co-Chair of the Radio Access Techniques of the 2006 IEEE VTC Fall 2006 and the Transmission Techniques of the IEEE VTC Fall 2012. From 2005 to 2008, he was the Chair of the IEEE Montreal Chapter in Communications and Information Theory. From 2020 to 2022, he was a Distinguished Lecturer of the IEEE Communications Society. He served as an Associate Editor for the IEEE COMMUNICATIONS LETTERS, IEEE TRANSACTIONS ON SIGNAL PROCESSING, and *IET Wireless Sensor Systems*. He currently serves as an Editor for the IEEE TRANSACTIONS ON COMMUNICATIONS, IEEE TRANSACTIONS ON VEHICULAR TECHNOLOGY, IEEE COMMUNICATIONS SURVEYS AND TUTORIALS, and IEEE WIRELESS COMMUNICATIONS LETTERS.

DEEMAH H. TASHMAN (Student Member, IEEE) received the B.Sc. and M.Sc. degrees (Hons.) in electrical engineering from the Jordan University of Science and Technology, Irbid, Jordan, in 2014 and 2017, respectively, and the Ph.D. degree in electrical and computer engineering from Concordia University, Montreal, QC, Canada, in 2022. She was a Research and a Teaching Assistant with the Jordan University of Science and Technology, Jordan, from 2014 to 2017, and Concordia University, from 2017 to 2022. Her research interests include the field of wireless communications, with emphasis on cooperative communications, multiple-input–multiple-output systems, physical-layer security, energy harvesting, and cognitive radio networks.

WALAA HAMOUDA (Senior Member, IEEE) received the M.A.Sc. and Ph.D. degrees in electrical and computer engineering from Queen's University, Kingston, ON, Canada, in 1998 and 2002, respectively. Since 2002, he has been with the Department of Electrical and Computer Engineering, Concordia University, Montreal, QC, Canada, where he is currently a Professor. From 2006 to 2015, he was the Tier II Concordia University Research Chair in communications and networking. He is currently the Tier I Concordia University Research Chair

JULES M. MOUALEU (Senior Member, IEEE) received the Ph.D. degree in electronic engineering from the University of KwaZulu-Natal, Durban, South Africa, in 2013. During his Ph.D. studies, he was a Visiting Scholar with Concordia University, Montreal, Canada, under the Canadian Commonwealth Scholarship Program (CCSP) offered by the Foreign Affairs and International Trade Canada (DFAIT). In 2015, he joined the Department of Electrical and Information Engineering, University of the Witwatersrand, Johannesburg, South Africa, where he is currently an Associate Professor. From 2018 to 2021, he was an Affiliate Assistant Professor with Concordia University. He is currently an NRF Y-Rated Researcher. His current research interests include cooperative and relay communications, cognitive radio networks, wireless body area networks, energy harvesting, massive multiple-input multiple-output systems, non-orthogonal multiple access schemes, and physical-layer security. He received the Exemplary Reviewer Award of the IEEE COMMUNICATIONS LETTERS, in 2018 and 2021, and the IEEE TRANSACTIONS ON COMMUNICATIONS, in 2021. He currently serves as an Associate Editor for IEEE ACCESS and *Frontiers in Communications and Networks*.

● ● ●